Biosensors and Bioelectronics 35 (2012) 376–381

Contents lists available at SciVerse ScienceDirect

Biosensors and Bioelectronics

journal homepage: www.elsevier.com/locate/bios

# Electrogenerated chemiluminescence biosensor incorporating ruthenium complex-labelled *Concanavalin A* as a probe for the detection of *Escherichia coli*

Haiying Yang[a,b], Yaqin Wang[a], Honglan Qi[a], Qiang Gao[a], Chengxiao Zhang[a,*]

[a] Key Laboratory of Applied Surface and Colloid Chemistry, Ministry of Education, School of Chemistry and Chemical Engineering, Shaanxi Normal University, Xi'an 710062, PR China
[b] Department of Chemistry, Yuncheng University, Yuncheng 044300, PR China

ARTICLE INFO

*Article history:*
Received 9 February 2012
Accepted 12 March 2012
Available online 30 March 2012

*Keywords:*
Biosensor
Electrogenerated chemiluminescence
*Escherichia coli*
*Concanavalin A*
Ruthenium(II) complex

ABSTRACT

A novel electrogenerated chemiluminescence (ECL) biosensor for highly sensitive detection of *Escherichia coli* (*E. coli*) was first developed by employing *Concanavalin* A (Con A) as a biological recognition element and bis(2,2′-bipyridine)-4′-methyl-4-carboxybipyridine ruthenium (II) (Ru1) complex as the detector. The ECL biosensor was fabricated by adsorbing carboxyl-functionalised single-wall carbon nanotubes (SWNTs) onto a paraffin-impregnated graphite electrode and further covalently coupling the Ru1–Con A probe onto the surface of the SWNT-modified electrode. Upon the binding of *E. coli* O157:H7 (as a model target), the biosensor showed a decreased ECL intensity in the presence of tri-*n*-propylamine (TPrA), which was in logarithmically direct proportion to the concentration of *E. coli* over a range from $5.0 \times 10^2$ to $5.0 \times 10^5$ cells/mL. The detection limit of this sensor was 127 cells/mL. Additionally, the ECL biosensor also showed satisfactory selectivity in discriminating gram-negative *E. coli* from gram-positive bacteria. The strategy developed in this study may be a promising approach and could be extended to the design of ECL biosensors for highly sensitive and rapid detection of other desired bacteria.



## 1. Introduction

Rapid methods for bacterial detection are essential in food, industrial and environmental monitoring, clinical diagnostics, and biodefence to allow faster decisions to be made with respect to food poisoning, water contamination, the presence of disease and, therefore, treatment options (Shen et al., 2007). *Escherichia coli* (*E. coli*) is one of the most common types of bacteria and is a normal inhabitant of the large intestine of warm-blooded animals. Some of the strains of *E. coli* are particularly virulent and, as is the case with *E. coli* O157:H7, cause a wide spectrum of human diseases Decludt et al. (2000). Most conventional methods for bacterial detection involving a selective enrichment step followed by biochemical screening and serological confirmation are time-consuming, often requiring 1–2 days to obtain results (Peter and Kristar, 2010). A rapid, quantitative, sensitive, and specific method for one-step detection of *E. coli* is therefore highly sought after.

Biosensors are simple, rapid and inexpensive analytical devices that promise to be useful tools for bacterial detection (Su et al., 2011). Extensive efforts have been devoted to the design of novel biosensors for bacterial detection, including the employment of novel biological recognition molecules as well as highly sensitive detectors and detection techniques. The recognition elements used in biosensors for bacteria involving *E. coli* O157:H7 mainly include antibodies, nucleic acid aptamers, or antimicrobial peptides and carbohydrates, which have an affinity for the epitopes present on the bacterial surface. The biosensors using different integrated detection techniques such as voltammetric (Emma and Evangelyn, 2011), potentiometric (Gustavo et al., 2010), impedimetric (Yang et al., 2004), or optical (Acharya et al., 2006) immunosensors, chemiluminescence aptasensors (Simon et al., 2011), fluorescence (Arcidiacono et al., 2008) or impedimetric (Mannoor et al., 2008) peptide-based biosensors, and quartz crystal microbalance (QCM) carbohydrate-based biosensors (Shen et al., 2007), have been developed for *E. coli* detection. However, the antibodies that are widely used have some limitations such as the challenging production of antibodies and antigens in vivo (O'Sullivan, 2002), and aptamers and antimicrobial peptides available for bacterial detections only have a limited numbers (Peter and Kristar, 2010).

Lectins, a group of proteins extracted from plants or animals, can strongly bind to specific carbohydrate moieties on the surface of bacteria (Nilsson, 2003; Sharon and Lis, 2004). Lectins are particularly interesting candidates for use as molecular recognition elements because of their ease of production and intrinsic stability. Electrochemical and optical biosensors for *E. coli* have been designed based on the importance of the interactions between lectins and glycoconjugates on bacterial cell surfaces (Hsu et al., 2006). Peter et al. (2003) reported lectin-based electrochemical biosensors to classify *E. coli* and other microbial species. Shen et al.

* Corresponding author. Tel.: +86 29 8153 0834; fax: +86 29 8153 0727.
*E-mail address:* cxzhang@snnu.edu.cn (C. Zhang).

0956-5663/$ – see front matter © 2012 Elsevier B.V. All rights reserved.
doi:10.1016/j.bios.2012.03.021

(2007) developed a QCM sensor utilising Con A as the recognition element for the detection of *E. coli* W1485 with a detection limit of 750 cells/mL. Recently, Gao et al. (2010) reported a resonant light scattering lectin array based on a sandwich model involving lectins as capture microbes and the gold nanoparticle-functionalised lectins as detectors for microbes, for example, with a linear response to *E. coli* DH5α ranging from $10^5$ to $10^8$ cells/mL. However, the lectin-based biosensors for *E. coli* reportedly suffer from a low sensitivity, and very little attention has been paid to the evaluation of the selectivity of the reported biosensors.

Electrogenerated chemiluminescence (ECL) biosensors are very promising due to their high sensitivity and ease of control (Miao, 2008; Zhang et al., 2008). Yu (2000) developed the ECL immunosensor using ruthenium complex-*E. coli* O157 antibody as the ECL probe and magnetic separation for the detection of *E. coli* O157 with a detection limit of 100 cells/mL. Daniel et al. (2004) also reported an ECL method for the estimation of *E. coli* O157 using ruthenium complex-polyclonal antibody as the ECL probe and enrichment step, which could detect one viable water-borne *E. coli* O157 in 100 mL of surface water. Recently, Han et al. (2011) reported an ECL competitive biosensor using mannan-functionalised CdS quantum dots as the ECL probe. Upon the competitive recognition of the immobilised mannan to Con A with a mannan-expressed BGC cell surface, the ECL intensity decreased due to the resistance of Con A. This biosensor showed a detection limit of $1.2 \times 10^3$ BGC cells/mL. However, the sensitivity of ECL biosensors without the enrichment and separation steps for bacteria should be improved. To the best of our knowledge, the ECL biosensor using promising lectin as the recognition element has not been reported.

With the foregoing analysis in mind, in this work, we describe a new and highly sensitive ECL biosensor for *E. coli* bacteria detection, in which the lectin Con A was selected as the recognition element. Using this ECL biosensor, the bioaffinity of Con A and *E. coli* (pathogenic and nonpathogenic strains) was also evaluated. The schematic diagram of the fabrication of the ECL biosensor and the ECL detection process is shown in Scheme 1. $Ru(bpy)_3^{2+}$ derivative-Con A was selected as the ECL probe. The biosensor was fabricated by covalently coupling the ECL probe on the surface of a paraffin-impregnated graphite electrode (PIGE) modified with carboxyl-functionalised carbon nanotubes. Upon binding of *E. coli* to the ECL probe to form a Con A-LPS conjugate, the change of ECL intensity was analyzed.

## 2. Materials and methods

### 2.1. Reagents and apparatus

*E. coli* O157:H7 (ATCC 35130) (heat-killed) was purchased from American Type Culture Collection (ATCC). *E. coli* DH5α, *E. coli* K12, *Micrococcus luteus* and *Staphylococcus aureus* were purchased from China Center of Industrial Culture Collection (Beijing, China). Millipore Milli-Q water (18.2 MΩ) was used. The reagents used in this work and the ECL experimental setup are provided in Supplementary data.

### 2.2. Synthesis of Ru1–Con A

The ECL probe Ru1–Con A (Supplementary data, Fig. S1) was synthesised following the method previously reported (Ewald et al., 1995) with a minor modification. Briefly, 50 μL of 2.4 μmol Ru1 dissolved in DMF was added to 1.5 mL of 0.20 M carbonate buffer (pH 8.5) containing 0.024 μmol Con A and allowed to stir gently free of light for 6 h at ~25 °C. The remaining unreacted Ru1 was separated from the Ru1–Con A using a Sephadex G-25 column. The fractions (14–20) were collected [Fig. S2(A)] as the probe solution and were stored at 4 °C before use.

### 2.3. Fabrication of the ECL biosensor

The PIGE (6.0 mm diameter) was polished on 400 grit SiC paper and then washed with water. SWNTs (10.0 mg) were ultrasonically dispersed in 10 mL of DMF, and then 10 μL of this dispersed suspension was drop-coated onto the surface of the pretreated PIGE and dried in air. The SWNT/PIGE was activated in 1 mL of freshly prepared solution containing 2 mg/mL EDC and 5 mg/mL NHS for 30 min and then rinsed with 10 mM PBS. The activated SWNT/PIGE was then immersed into 100 μL of 20 μM Ru1–Con A for 1 h at ~25 °C. After rinsing with 10 mM PBS, the electrode was soaked in 1% BSA for 30 min to block the surface active sites of the SWNT/PIGE. Finally, the ECL biosensor was rinsed with 10 mM PBS and stored at 4 °C in the dark.

### 2.4. ECL measurement

The ECL biosensor was immersed in 100 μL of a fixed concentration of *E. coli* O157:H7 for an incubation time of 60 min, then rinsed with 10 mM PBS. The ECL measurement was performed in 2 mL of 100 mM TPrA at a constant potential of +1.35 V. The concentration of *E. coli* was quantified by a decreased ECL intensity $\Delta I$ ($\Delta I = I_0 - I$), where $I_0$ and $I$ are the integrated ECL intensity before and after incubation with *E. coli*, respectively. The integrated time was 30 s.

## 3. Results and discussion

### 3.1. UV-Vis and ECL characterisation of the ECL probe

The synthesised ECL probe Ru1–Con A was characterised by UV-Vis spectrometry and sodium dodecyl sulphate-polyacrylamide gel electrophoresis (SDS-PAGE). Compared with the absorption spectra of Con A and Ru1, the absorption spectrum of Ru1–Con A [curve c in Fig. S2(B)] showed a broad peak at ~454 nm, which was assigned to the characteristic absorption peak of Ru1, and a maximum peak at 287 nm, which was assigned to a combination of the characteristic absorption peaks of Ru1 and Con A. We inferred that the absorption peak at 287 nm (slightly blue-shifted) originated from $n \rightarrow \pi^*$ transitions of the amido bond formed through linking the carbonyl moiety of Ru1 with the amido group of Con A (Zhang et al., 2008), indicating that Ru1 was successfully coupled to Con A. From the SDS-PAGE image, one band at approximately 25 kDa was clearly observed for Ru1–Con A (Fig. S3, lane 2 to lane 4). This band was slightly higher than the same band of native Con A (25 kDa), the shift attributed to the band of Con A monomer labelled as Ru1. Furthermore, the labelling ratio of Ru1–Con A was estimated to be 4:1 based on the absorbance values at 454 nm for Ru(II) and at 280 nm for Con A, suggesting that Ru1 was coupled to Con A via an acylation reaction of the amino group of Lys 114 on Con A with the carboxylate moiety of Ru1 (Eiji et al., 2005).

The ECL behaviour of Ru1–Con A was investigated at a PIGE electrode using a linear potential scan technique. Fig. 1 shows ECL intensity-potential profiles of Ru1 and the ECL probe. The ECL peak of Ru1 appears at +1.32 V ($I_{max}$ = 39,710) and that of Ru1–Con A appears at +1.35 V ($I_{max}$ = 6899), indicating that the ECL behaviour of the probe is similar to the ECL behaviour of Ru1. The ECL intensity of Ru1 is nearly six times higher than the ECL intensity of Ru1–Con A at the same Ru1 content, which means that the ECL efficiency of Ru1 labelled on Con A is ~17% of that obtained from free Ru1 because the size of Ru1–Con A is much larger than the size of the Ru1 and the diffusion coefficient of Ru1–Con A is smaller than the diffusion coefficient of the Ru1 in solution. The ECL from Ru1–Con

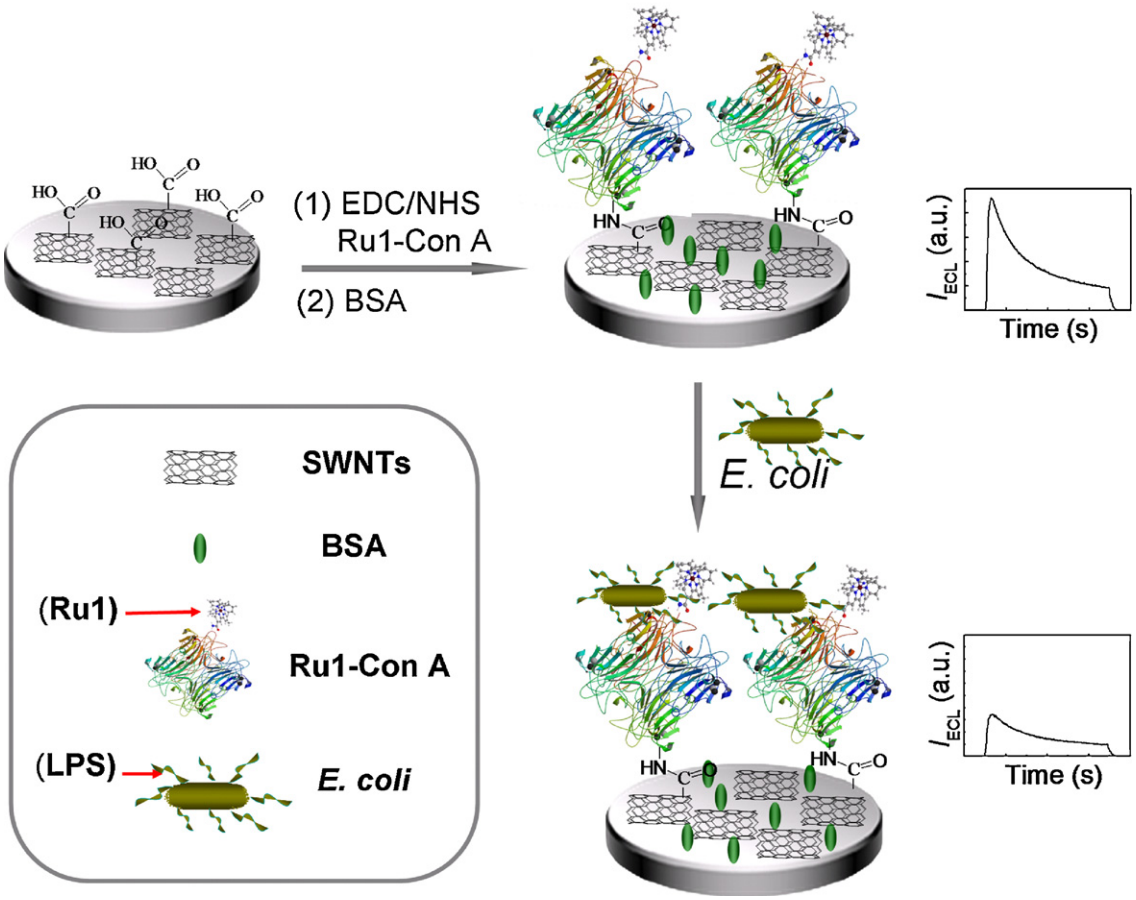


**Scheme 1.** Schematic diagram of ECL biosensor fabrication and *E. coli* detection.

A is generated at a slightly positive potential (~30 mV) compared with the potential of free Ru1.

### 3.2. Optimisation of fabrication and detection conditions

To monitor each immobilisation step and binding step, corresponding impedance spectra were recorded (Fig. S4). The results showed that when the ECL probe was immobilised on the SWNT/PIGE, the interaction between Con A and *E. coli* DH5α occurred, and the fabricated sensor could work successfully. The ECL kinetic profiles of the ECL biosensors fabricated before and after interaction with *E. coli* strains DH5α and O157:H7 (Fig. S5) showed that the ECL intensity ($I$) decreased from 199,012 to 133,240 when the *E. coli* DH5α concentration was elevated from $5.0 \times 10^2$ to $5.0 \times 10^3$ cells/mL, compared with ECL intensity before incubation ($I_0$ = 263,820, a.u.). The decrease of the ECL intensity may be attributed to the following three factors. First, *E. coli* DH5α bound to Ru1–Con A on the biosensor surface inhibits the electron transfer reactions, including the oxidation of TPrA to $TPrA^{\bullet+}$ and the oxidation of $Ru(bpy)_3^{2+}$ to $Ru(bpy)_3^{3+}$ on the surface of the electrode, thereby leading to a reduction in the amount of the excited-state $Ru(bpy)_3^{2+*}$ (Miao, 2008). Second, the micro-environment of ECL centre Ru1 changed upon binding the *E. coli* because Ru1 was tethered at Lys 114 in the proximity of the sugar-binding site of Con A (Nagase et al., 2003). Third, the $Ru(bpy)_3^{2+*}$ could be partly eliminated by the conjugate complex of *E. coli* DH5α bound to the Ru1–Con A on the biosensor surface, in a manner similar to luminescence quenching (Ramanavicius et al., 2010). Additionally, a nearly similar signal change was observed for these two strains, indicating that the fabricated ECL biosensor can respond to *E. coli* O157:H7 and *E. coli* DH5α. The ECL kinetic profile showed that the ECL intensity reached a peak in less than 2 s and had nearly decayed to background in less than 30 s. Therefore, the integrated ECL intensity from 30 s from the beginning of the applied potential was used as the ECL intensity to quantify the concentration of *E. coli*.

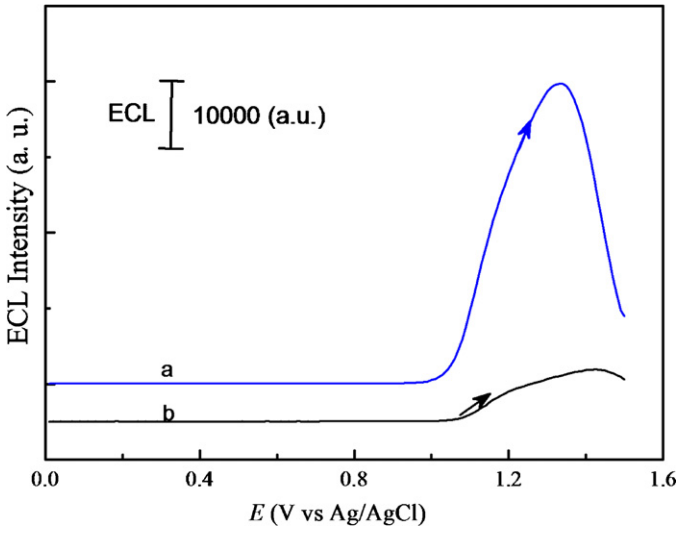


**Fig. 1.** The ECL potential profiles obtained in 0.10 M TPrA with a scan rate of 100 mV/s. (a) 0.64 μM Ru1; and (b) 0.16 μM Ru1–Con A.

Considering the toxicity of *E. coli* O157:H7 and the experimental result described above, we employed a nonpathogenic strain of *E.*

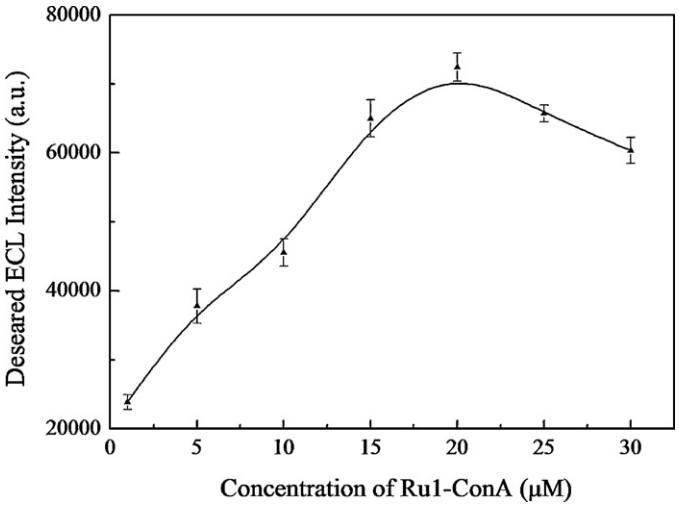


**Fig. 2.** Dependence of the ECL intensity on the concentration of the ECL probe after incubation with $5 \times 10^3$ cells/mL of *E. coli* DH5α with an incubation time of 60 min. The ECL measurement was carried out in 0.10 M TPrA. The applied potential was at +1.35 V.

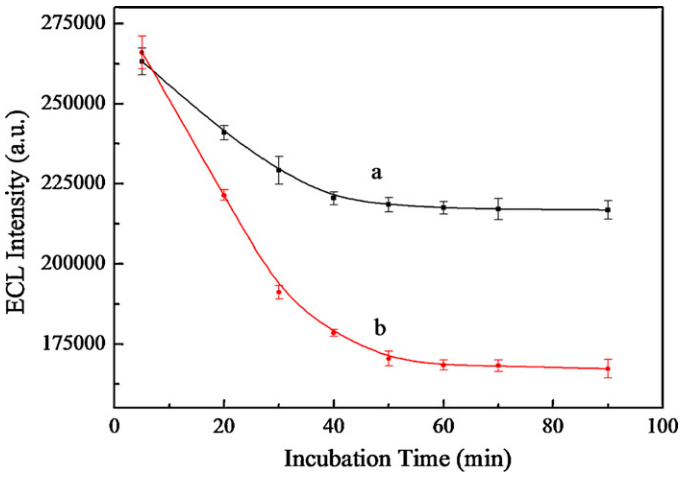


**Fig. 3.** Effect of incubation time on the ECL intensity after incubation with *E. coli* DH5α. (a) $5 \times 10^2$ cells/mL; and (b) $5 \times 10^3$ cells/mL. ECL measurement conditions were the same as in Fig. 2.

*coli* DH5α as a surrogate for O157:H7 to optimise the fabrication and detection conditions (Gustavo et al., 2010). To check the effect of SWNTs on the ECL intensity, two ECL biosensors of Ru1–Con A/SWNTs/PIGE and Ru1–Con A/PIGE were fabricated. The Ru1–Con A/PIGE was fabricated, on the basis of physical adsorption, by immersing the PIGE into 100 μL of 20 μM Ru1–Con A for 1 h, while Ru1–Con A/SWNTs/PIGE was fabricated as described in Section 2.3. The result showed that the ECL intensity of Ru1–Con A/SWNTs/PIGE ($I_0$ = 287,796) was approximately seven times higher than the ECL intensity of Ru1–Con A/PIGE ($I_0$ = 39,710) without incubation with *E. coli* DH5α. When the two biosensors were incubated with $5.0 \times 10^3$ cells/mL *E. coli* DH5α, the Ru1–Con A/SWNTs/PIGE biosensor gave a much higher ECL response ($\Delta I$ = 106,542) than the Ru1–Con A/PIGE biosensor ($\Delta I$ = 14,063). In other word, $\Delta I$ of Ru1–Con A/SWNTs/PIGE was approximately seven times higher than $\Delta I$ of Ru1–Con A/PIGE, indicating that SWNTs can greatly increase the ECL response. The increase in ECL response occurred because SWNTs increase the immobilised amount of the ECL probes on the PIGE due to the large surface area of SWNTs (Alan et al., 2011) while the ECL probes attached to PIGE by physical adsorption could easily be washed away (Jeykumari and Narayanan, 2008). SWNTs were therefore used as a substrate for the fabrication of the ECL biosensor to enhance the sensitivity of the ECL biosensor.

The concentration of the ECL probe for the fabrication of the biosensor directly influences the surface coverage of the ECL probe on SWNTs/PIGE for bacterial detection. Fig. 2 shows that $\Delta I$ decreases nearly linearly with the increment of the ECL probe concentration from 1 to 20 μM because the surface coverage of the ECL probe increases. Then, $\Delta I$ increases with the increment of the ECL probe concentration from 20 to 30 μM because the highly condensed surface coverage of the ECL probe could sterically hinder the ECL reaction and the binding of immobilised Con A with *E. coli* DH5α. The 20 μM ECL probe was therefore used to obtain a high sensitivity.

Important detection conditions including applied potential and incubation time were optimised. The influence of the applied potential (+0.5 to +1.5 V) on the ECL intensity was examined in the absence and presence of $5 \times 10^3$ cells/mL *E. coli* DH5α. The $I_0$ and $\Delta I$ showed similar trends and sharply increased when the applied potential increased from +0.8 V to +1.20 V (data not shown) because TPrA is oxidised at $E_p$ = +0.9 V and Ru1 is oxidised at $E_p$ = +1.1 V. The $I_0$ and $\Delta I$ increased slightly when the applied potential increased from +1.20 V to +1.35 V and reached a maximum at approximately +1.35 V (Fig. S6). Experimentally, +1.35 V was found to be the optimal potential. A positive potential shift of 0.25 V from the reversible redox potential of $Ru(bpy)_3^{2+}$ in solution could result from the effect of the electrode material (i.e., PIGE vs. GCE) as well as the minor electronic resistance between the PIGE and Ru1 redox centres because of the protein Con A, which hinders the electron transfer. However, $I_0$ decreases with a further increase of the applied potential. The reason for the decrease of $I_0$ beyond +1.35 V remains unclear but could be related to the oxidation of water that produces extra amounts of oxygen, resulting in the consumption of TPrA• radicals needed for the generation of the $Ru1^{2+*}$ species (Zheng and Zu, 2005). After incubation with *E. coli*, the ECL intensity and $\Delta I$ showed the same variation in trend as before incubation. Therefore, a constant potential of +1.35 V was chosen to obtain a high sensitivity.

Incubation time was also an important parameter for the kinetic binding between Con A and *E. coli*. Fig. 3 shows the dependence of the ECL intensity on the incubation time. Without incubation of the *E. coli* DH5α, the ECL intensity maintained a constant value (data not shown). The ECL intensity decreased sharply with an increase of the incubation time from 5 min to 30 min. A 50% decrease of the ECL intensity was observed approximately 20 min after incubation with $5 \times 10^3$ cells/mL *E. coli* DH5α (curve b in Fig. 3), and a steady state was reached after 50 min, while an ~50% decrease of the ECL intensity appeared after ~25 min, and a steady state is reached after 50 min for $5 \times 10^2$ cells/mL *E. coli* DH5α (curve a in Fig. 3). These results suggest that the initial binding reaction proceeded quickly, and the binding reaction was completed in ~60 min, which is in accordance with a value of 60 min between Con A in solution and carbohydrates immobilised on an ECL biosensor (Han et al., 2011). To ensure the binding efficiency and rapid detection of *E. coli*, an incubation time of 60 min was chosen in the following experiments.

### 3.3. Performance of the ECL biosensor for E. coli

The quantitative behaviour of the ECL biosensor was assessed by measuring the dependence of $\Delta I$ upon the concentration of *E. coli* O157:H7 (Fig. 4) and *E. coli* DH5α (Fig. S7) under the optimised conditions. The results showed that $\Delta I$ was logarithmically in direct proportion to the concentration of *E. coli* O157:H7 in the range from $5.0 \times 10^2$ to $5.0 \times 10^5$ cells/mL. The linear regression equation was $\Delta I = 209{,}82 \lg C - 19{,}844$ (*C*: cells/mL) with a

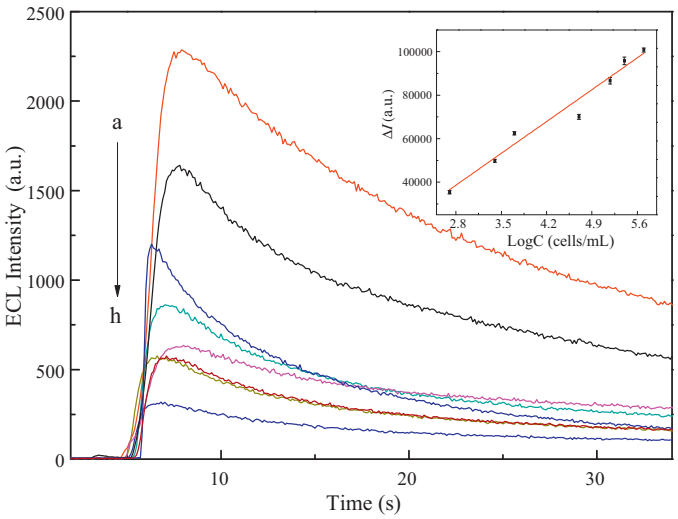


**Fig. 4.** The ECL profiles of the biosensor after incubation with *E. coli* O157:H7 at concentrations of 0, $5.0 \times 10^2$, $2.5 \times 10^3$, $5.0 \times 10^3$, $5.0 \times 10^4$, $1.5 \times 10^5$, $2.5 \times 10^5$, and $5.0 \times 10^5$ cells/mL (from a to h) with an incubation time of 60 min. ECL measurement conditions were the same as in Fig. 2.

coefficient of 0.9647. The detection limit was calculated to be 127 cells/mL O157:H7 based on a signal-to-noise ratio of 3. The detection limit was approximately fivefold lower than the value of 750 cells/mL *E. coli* at a QCM biosensor for *E. coli* W1485 using Con A as the recognition element (Shen et al., 2007), eightfold lower than the value of 1000 CFU/mL *E. coli* O157:H7 obtained from a peptide-based impedimetric biosensor (Mannoor et al., 2008) and slightly lower than 136 cells/mL *E. coli* O157:H7 obtained from a DNA-based chemiluminescence biosensor (Simon et al., 2011). The calculated detection limit of 127 cells/mL nearly reached the detection limit of 100 cells/mL *E. coli* O157:H7 obtained from an ECL immunosensor with a magnetic enrichment process (Yu, 2000). The high sensitivity obtained in our work may be ascribed to employing Con A as the molecular recognition element and Ru1 as the signal-producing compound as well as SWNTs as amplification substrates.

The reproducibility of the ECL biosensor was also estimated by testing $5.0 \times 10^3$ cells/mL *E. coli* DH5α three times with five biosensors and by performing seven independent measurements with one ECL biosensor. The relative standard deviation obtained was 4.8% for the five biosensors and 3.6% for the seven independent measurements.

### 3.4. Evolution of the selectivity of the ECL biosensor

The selectivity of the Con A-based biosensors was assessed by testing other bacteria (at the concentration of $5.0 \times 10^3$ cells/mL) including gram-negative pathogenic *E. coli* O157:H7 and *E. coli* K12, nonpathogenic *E. coli* DH5α, gram-positive nonpathogenic *Micrococcus luteus*, and gram-positive pathogenic *Staphyolcoccus aureus*. The results showed that $\Delta I$ for *E. coli* K12 and $\Delta I$ for *E. coli* DH5α were 95.8% and 101%, respectively, of the $\Delta I$ for *E. coli* O157:H7. $\Delta I$ values for *Micrococcus luteus* and *Staphyolcoccus aureus* were only 13.1% and 15.3%, respectively, of the $\Delta I$ value for *E. coli* O157:H7. All these results suggested that the ECL biosensor possessed high responsive to *E. coli* strains and could be employed to discriminate the gram-negative bacteria *E. coli* from the tested gram-positive bacteria. The possible reason may be that LPS is the major component of the outer membrane for gram-negative bacteria but not for gram-negative bacteria. The response of different *E. coli* strains varied slightly, possibly because LPS *O*-antigens are unique to specific bacterial strains (Peter et al., 2001). Intriguingly, this result agrees with the previous report that the Con A-based biosensor could detect gram-negative bacteria

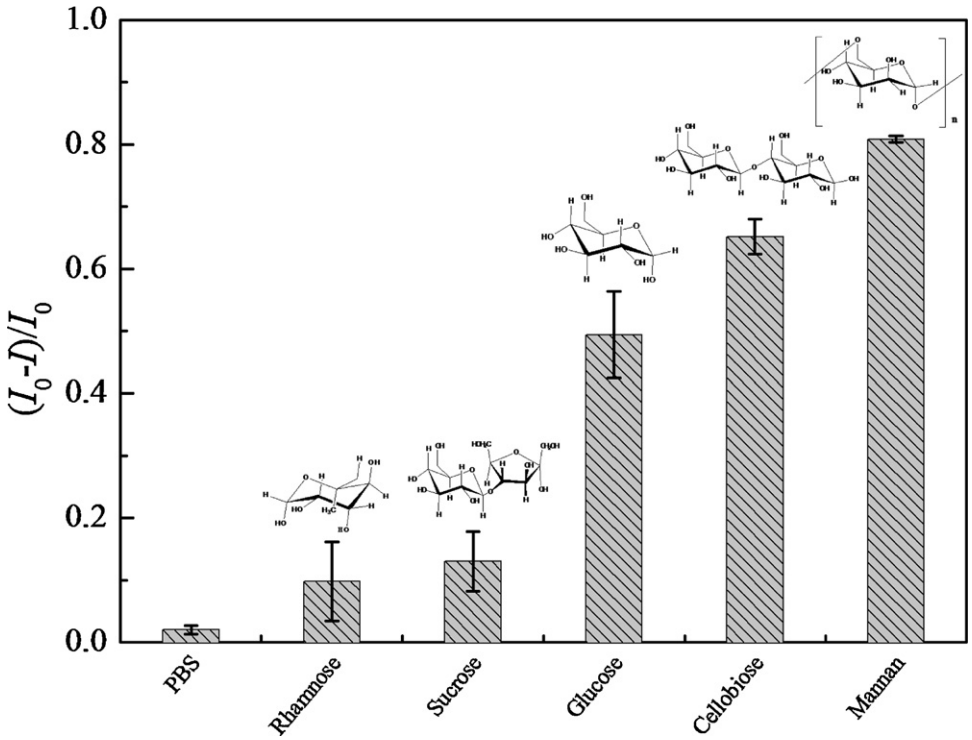


**Fig. 5.** The ECL responses of the biosensor to carbohydrates. The concentration of carbohydrate was 0.1 nM, and the incubation time was 60 min. ECL measurement conditions were the same as in Fig. 2.

*E. coli* W1485 rather than gram-positive bacteria (Shen et al., 2007). Unfortunately, the biosensor in this work could not selectively respond to pathogenic *E. coli* O157:H7 among the *E. coli* strains. The presence of *E. coli*, even nonpathogenic strains, is evidence of recent contamination and provides sufficient grounds to quarantine the water source for further investigation (WHO, 2004; Emma and Evangelyn, 2011).

To demonstrate the plausibility of evaluating drinking water samples using our biosensor, the recovery of *E. coli* O157:H7 from tap water was tested by spiking samples with *E. coli* O157:H7 to attain final concentrations of $5.0 \times 10^3$ cells/mL and $5.0 \times 10^4$ cells/mL (Ehsan et al., 2008). The recovery was assessed to be 95% for $5.0 \times 10^3$ cells/mL and 89% for $5.0 \times 10^4$ cells/mL, indicating that the developed sensor could potentially detect *E. coli* in samples.

In an attempt to further evaluate the selectivity of the biosensor, a panel of carbohydrates was tested, including the specific binding carbohydrates (glucose and mannose) and nonspecific carbohydrates (galactose and rhamnose). The results are shown in Fig. 5. $\Delta I$ was 40% for glucose and 51% for mannose. In stark contrast, $\Delta I$ was only 8% for galactose and 6% for rhamnose because the binding activity of Con A extends only towards the presence of vicinal, equatorial hydroxyl groups in the carbohydrate stereochemistry of the 3-OH and 4-OH carbohydrates such as glucose and mannose (Sandeep et al., 2009). Hence, Con A rarely binds to galactose and rhamnose because these two carbohydrates have an axial 4-OH, possessing a fundamentally different stereochemistry. $\Delta I$ for mannan (81%) was larger than $\Delta I$ for mannose (51%), ascribed to a high binding affinity of Con A towards mannan for the multivalent interaction. To further understand the binding of Con A and *E. coli*, the binding constant ($K$) of the immobilised Ru1–Con A with mannan was determined using the proposed ECL method (Sun et al., 2010) to be $5.2 \times 10^{10}\ M^{-1}$ from the plot of $C_m/\Delta I$ as a function of $C_m$ representing a Langmuir adsorption isotherm (where $C_m$ is the mannan concentration) (Fig. S8). This value is slightly higher than $5.3 \times 10^9\ M^{-1}$ obtained by SPR for yeast mannan and Con A (Jana et al., 2004). This large $K$ value suggests that the binding strength between mannan and the surface-confined Con A is significantly strong.

## 4. Conclusion

A highly sensitive ECL biosensor for *E. coli* detection has been developed by employing the lectin Con A as the recognition element and a ruthenium (II) complex as the reporting element. It was found that Con A tended strongly towards *E. coli* strains and could be utilized to discriminate gram-negative *E. coli* from the tested gram-positive bacteria. The low detection limit was 127 cells/mL for *E. coli* O157:H7 and the assay (including incubation and detection time for *E. coli*) could be completed in 70 min. The strategy proposed is a promising approach and provides a significant positive impact on the use of ECL biosensors in potential applications. However, a number of challenges remain in achieving the final target of highly selective and sensitive detection of *E. coli* O157:H7. Lectins that are highly selective towards *E. coli* O157:H7 should be pursued, and lectin-based arrays should be developed. Additionally, a detection limit that achieves the required value in real samples should be also pursued. Based on our previous work in coupling the ECL probe to a dendrimer (Ma et al., 2012) or nanomaterials such as gold nanoparticles and carbon nanotubes, significantly enhanced sensitivity may be achievable.

## Acknowledgments

Financial support from the National Science Foundation of China (No. 20975065) and Innovation Funds for Graduate Programs of Shaanxi Normal University (No. 2011CXB010) are gratefully acknowledged.

## Appendix A. Supplementary data

Supplementary data associated with this article can be found, in the online version, at doi:10.1016/j.bios.2012.03.021.

## References

Acharya, G., Chang, C., Savran, C., 2006. J. Am. Chem. Soc. 128, 3862–3863.
Alan, L.G., Michael, H., Serge, C., 2011. Analyst 136, 1279–1287.
Arcidiacono, S., Pivarnik, P., Mello, C.M., Senecal, A., 2008. Biosens. Bioelectron. 23, 1721–1727.
Daniel, R.S., James, A.H., Joann, S.V.K., Yakov, A.P., Kenneth, B., Jeffrey, S.K., 2004. J. Microbiol. Methods 58, 223–231.
Decludt, B., Bouvet, P., Mariani-Kurkdjian, P., Grimont, F., Grimont, P.A., Hubert, B., Loirat, C., 2000. Epidemiol. Infect. 124, 215–220.
Eiji, N., Yoichiro, K., Erina, K., Yoshiki, K., Itaru, H., 2005. J. Am. Chem. Soc. 127, 13253–13261.
Ehsan, M., Keith, B.M., John, H.T.L., 2008. J. Agric. Food Chem. 56, 7691–7695.
Emma, B.S., Evangelyn, C.A., 2011. Biosens. Bioelectron. 26, 2208–2214.
Ewald, T., Henryk, S., Henryk, M., Joseph, R.L., 1995. Biophys. J. 68, 342–350.
Gao, J., Liu, D., Wang, Z., 2010. Anal. Chem. 82, 9240–9247.
Gustavo, A.Z.G., Suryakant, V.B., Bhosale, J.R., Rius, F.X., 2010. Anal. Chem 82, 9254–9260.
2004. Guidelines for Drinking-Water Quality, 3rd ed. World Health Organization.
Han, E., Ding, L., Jin, S., Ju, H.X., 2011. Biosens. Bioelectron. 26, 2500–2505.
Hsu, K.L., Pilobello, K.T., Mahal, L.K., 2006. Nat. Chem. Biol. 2, 153–157.
Jana, M., Estera, S.D., Jenny, C., Bengt, D., 2004. J. Biochem. Biophys. Methods 60, 163–170.
Jeykumari, D.R.S., Narayanan, S.S., 2008. Biosens. Bioelectron. 23, 1404–1411.
Ma, F., Zhang, Y., Qi, H., Gao, Q., Zhang, C., Miao, W., 2012. Biosens. Bioelectron. 32, 37–42.
Mannoor, M.S., Zhang, S., Link, A.J., McAlpine, M.C., 2008. Proc. Natl. Acad. Sci. USA 45, 19207–19212.
Miao, W., 2008. Anal. Chem. 108, 2506–2553.
Nagase, T., Nakata, E., Shinkai, S., Hamachi, I., 2003. Chem. Eur. J. 9, 3660–3669.
Nilsson, C.L., 2003. Anal. Chem. 75, 348A–353A.
O'Sullivan, C.K., 2002. Anal. Bioanal. Chem. 372, 44–48.
Peter, E., Melany, W., Eduardo, C., Susan, R.M., 2003. Biosens. Bioelectron. 18, 907–916.
Peter, J.V., Kristar, W., 2010. Environ. Sci. Technol. 44, 3656–3669.
Peter, E., Susan, R.M., 2001. Anal. Chem. 73, 4241–4248.
Ramanavicius, A., Ryskevic, N., Oztekin, Y., Kausaite-Minkstimiene, A., Jursenas, S., Baniukevic, J., Kirlyte, J., Bubniene, U., Ramanaviciene, A., 2010. Anal. Bioanal. Chem. 398, 3105–3113.
Sandeep, K., Debasisa, M., Avadhesha, S., 2009. Biophys. J. 96, 21–34.
Sharon, N., Lis, H., 2004. Glycobiology 14, 53R–62R.
Shen, Z., Huang, M., Xiao, C., Zhang, Y., Zeng, X., Wang, P.G., 2007. Anal. Chem. 79, 2312–2319.
Simon, C.D., Reinhard, N., Michael, S., 2011. Anal. Chem. 83, 3153–3160.
Su, L., Jia, W., Hou, C., Yu, L., 2011. Biosens. Bioelectron. 26, 1788–1799.
Sun, B., Qi, H., Ma, F., Gao, Q., Zhang, C., Miao, W., 2010. Anal. Chem. 82, 5046–5052.
Yang, L., Li, Y., Erf, G.F., 2004. Anal. Chem. 76, 1107–1113.
Yu, H., 2000. Biosens. Bioelecton. 14, 829–840.
Zhang, J., Qi, H., Li, Y., Yang, J., Gao, Q., Zhang, C., 2008. Anal. Chem. 80, 2888–2894.
Zheng, H., Zu, Y., 2005. J. Phys. Chem. B 109, 12049–12053.